2015 IEEE International Conference on Robotics and Automation (ICRA)
Washington State Convention Center
Seattle, Washington, May 26-30, 2015

Asynchronous Blind Signal Decomposition Using Tiny-Length Code for Visible Light Communication-Based Indoor Localization

Fangyi Zhang, Kejie Qiu, Ming Liu
The Hong Kong University of Science and Technology
{eezhangfy, kqiuaa, eelium}@ust.hk

***Abstract*—Indoor localization is a fundamental capability for service robots and indoor applications on mobile devices. To realize that, the cost and performance are of great concern. In this paper, we introduce a lightweight signal encoding and decomposition method for a low-cost and low-power Visible Light Communication (VLC)-based indoor localization system. Firstly, a Gold-sequence-based tiny-length code selection method is introduced for light encoding. Then a correlation-based asynchronous blind light-signal decomposition method is developed for the decomposition of the lights mixed with modulated light sources. It is able to decompose the mixed light-signal package in real-time. The average decomposition time-cost for each frame is 20 ms. By using the decomposition results, the localization system achieves accuracy at 0.56 m. These features outperform other existing low-cost indoor localization approaches, such as WiFiSLAM.**

I. Introduction

A. Motivation

Indoor localization is fundamental for various robotic and intelligent device-based applications. Although research on this topic has been conducted for a long time, there are still many unsolved practical problems, especially the balance of cost reduction and performance improvement. Most of existing approaches reach a high accuracy with costly exteroceptive sensors, such as cameras [1], [2], [3], [4] and range-finders [5]. Even though WiFiSLAM [6], [7] can provide a low-cost solution, its application scope is very limited due to relatively low precision and sensitivity to noise.

WiFiSLAM utilizes radio-frequency beacons in the environments. Inspired by this and Visible Light Communication (VLC) [8], [9], a VLC-based indoor localization framework was preliminarily proposed in our previous work [10]. It aims at low-cost localization with higher precision than WiFiSLAM. To achieve the aim, more in-depth research is necessary.

B. VLC-based Indoor Localization System

The entire system includes hardware and software. The hardware system consists of two major parts: modulated LED light sources and a photonic diode. The modulated LED light sources are used to construct a space illuminated with beacons. All the LED lights are modulated with selected beacon codes (following the algorithm defined in Section II) and work at the same frequency (960 Hz) in rectangle waveforms. The beacons are not observable by human eyes due to the high frequency; however, they are observable by a photonic sensor. The photonic sensor can then localize based on the "fingerprints" of locations. For further references to our hardware system, please check our previous report [10].

Once the light field is determined, the localization is achieved by a series of processes, including three major parts: light-signal decomposition, Gaussian-Process-Regression (GPR)-based map generation, and Bayesian filter-based localization as shown in Fig. 1. The signal decomposition component decomposes the received light-signal and computes the received intensity for each source. These intensities and the corresponding locations are fed into the GPR-based map generation component, such that mean maps and variance maps are constructed as shown in Fig. 1. Using these outputs, localization is achieved through the Bayesian filter-based localization component. We mainly deal with the light-signal decomposition in this paper. For the readers that are interested in the map generation and localization, please refer to our future reports.

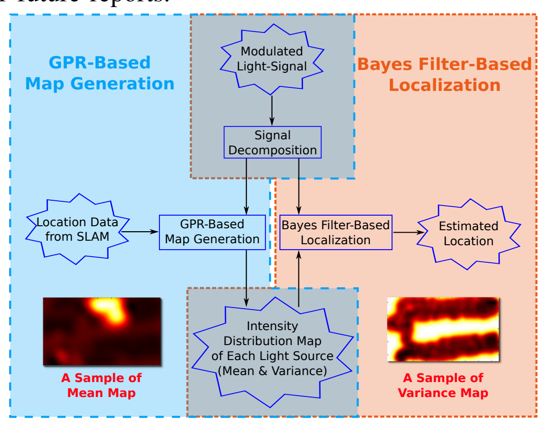

Fig. 1. Localization software framework

C. Challenges and Contributions

The decomposition method introduced in our previous report [10] needs synchronisation in the light sources side. However, in real applications, synchronisation of a large number of modulated light sources at sub-microsecond precision is very difficult or costly to achieve. So asynchronous light-signal decomposition is necessary. Lights that are modulated with different beacon codes will be additively mixed together with random phases as input to the photonic sensor, i.e., a mixture of blind signals which is difficult to process. Its decomposition is sensitive to noise. Although the accuracy and stability of the light-signal decomposition might be improved by lengthening the beacon codes, it will largely increase the calculation cost of the decomposition and jeopardize the real-time performance.

Therefore, an effective short codes selection method and corresponding efficient decomposition algorithm are required.

This work was partially supported by the HKUST Project IGN13EG03; partially sponsored by the Research Grant Council of Hong Kong SAR Government, China, under project No. 16206014 and National Natural Science Foundation of China No. 6140021318. All projects are awarded to Prof. Ming Liu.

We address the following two major contributions:

1) An algorithm for tiny-length code selection: is developed to get suitable 31-bit Gold-sequences. It is named *tiny-length*, because the shortest code for existing CDMA standard is 127 bits, which is four times longer. Even with yet low signal-to-noise ratio, the 127-bit codes are already too timely costly for the VLC system with a 960 Hz base-frequency (due to hardware constraints). In this work, the beacon codes selected by the proposed algorithm are with not only optimal correlation properties but also balanced energy. They are suitable for the correlation-based asynchronous blind signal decomposition. The generated codes can also be used as references for other similar problems, such as RF-based localization.

2) A low-cost light-signal decomposition algorithm: is developed to deal with the asynchronous blind light-signal decomposition. The decomposition is realized by correlation analysis. It can accurately and stably extract the intensity of each received beacon component. The average decomposition time-cost per frame is 20 ms.

D. Organization

For the remainder of the paper, in Section II, the code selection algorithm is introduced. The signal decomposition algorithm is then discussed in Section III. In Section IV and Section V, the validation experiments and localization tests are introduced, respectively. At the end, we conclude our work and make an outlook for the work that could be done in the future.

II. Beacon Code Selection

A. Pseudonoise (PN) Sequences

The proposed method is partially based on an existing PN-sequence framework. For the asynchronous blind signal decomposition, the most widely used PN-sequences are: maximal length sequence (m-sequence), Gold-sequence and Kasami-sequence. They all claimed to have very low cross-correlation and good auto-correlation, especially for long-length codes. Their unique characteristics including correlation functions are discussed in [11], [12], [13], [14], [15], [16].

The cross-correlation response of m-sequence can be unexpectedly high in some special cases [12]. The unexpected high response is bad for the light-signal decomposition. But for Gold-sequence and Kasami-sequence, their correlation responses can only be several specific values in constrained ranges [13], [14]. For the VLC-based indoor localization system, we need a large number of tiny-length beacon codes with low cross-correlation responses. Therefore, both Gold-sequence and Kasami-sequence are potential optimal choices, except m-sequence.

B. Cross-correlation Performance of Different PN-sequences

According to the correlation functions of Gold-sequence and Kasami-sequence discussed in [13] and [14], possible correlation responses are discussed here. The correlation functions in [13] and [14] are for PN-sequences in the form of "-1" and "1" ("(-1)-1" binary form). But in the VLC system, the beacon codes are transmitted through lights in the form of on and off, where the form of "0" and "1" ("0-1" binary form) can better indicate the energy cases. In this paper, the encoding and decomposition of light-signals are in "0-1" binary form.

For our specific case (all beacon codes are balanced; guaranteed by the algorithm in Section II-D), the relation between the above two forms is $R_{a',b'} = \frac{1}{4}R_{a,b} + \frac{1}{2} + \frac{L}{4}$, where $R_{a,b}$ and $R_{a',b'}$ are the respective cross-correlation responses of two codes in "(-1)-1" binary form (C_a, C_b) and "0-1" binary form ($C_{a'}, C_{b'}$). L is the code length. Detail inference will be introduced in our future reports.

The computed cross-correlation peak and least values as well as corresponding amount of available sequences are listed in Table I for each kind of PN-sequence (L between 15 and 4095). The cross-correlation values are normalized values. The normalized auto-correlation values are all 1. "-" denotes that there is no available data.

In Table I, there is no available data for Kasami-sequences with the lengths of 31, 127, 511 and 2047, since there is no available Kasami-sequence with these lengths [14]. Although the peak and least values of each small-set Kasami-sequence (L=15, 255, 4095) are respectively closer to zero than those of corresponding Gold-sequence, its amount of available sequences is much less than that of Gold-sequence. For each large-set Kasami-sequence (L=63, 1023), although the amount is much larger than that of Gold-sequence, their peak and least values are respectively same.

TABLE I
Cross-Correlation Performance Indicators

	Peak Value		**Least Value**		**Amount**		N^*	
$L/bits$	Gold	Kasami	Gold	Kasami	Gold	Kasami	Gold	Kasami
15	0.7500	0.6250	0.2500	0.3750	17	4	1	2
31	**0.6250**	-	**0.3750**	-	**33**	-	**2**	-
63	0.6250	0.6250	0.3750	0.3750	65	520	2	2
127	0.5625	-	0.4375	-	129	-	4	-
255	0.5625	0.5312	0.4375	0.4687	257	16	4	8
511	0.5313	-	0.4687	-	513	-	8	-
1023	0.5313	0.5313	0.4688	0.4688	1025	32800	8	8
2047	0.5156	-	0.4844	-	2049	-	16	-
4095	0.5156	0.5078	0.4844	0.4922	4097	64	16	32

C. The Optimal Type and Length of Beacon Codes

With suitable beacon codes, the correlation response between the mixed signal and the included beacon code with the highest intensity (with a right phase) is usually greater than that for a certain irrelevant beacon or irrelevant phase. This is the basis of our light-signal decomposition algorithm. However, the response for a certain irrelevant beacon might be incidentally the peaked correlation response (Incidental Case). To guarantee high enough reliability of the decomposition, the occurrence rate of this case should be reduced by maximizing the difference between auto-correlation and cross-correlation, or through limiting the amount of mixed beacon codes.

The maximum allowed amount (N^*) of mixed beacon codes can be theoretically represented as

$$N^* = \frac{1 - Normalize(R^*_{m,n})}{Normalize(R^{-}_{m,n}) - Normalize(R^*_{m,n})} \qquad (1)$$

where $R^{-}_{m,n}$ and $R^*_{m,n}$ are the peak and least values (listed in Table I) of $R_{m,n}$, respectively. $R_{m,n}$ is the correlation response of any PN-sequences m and n (with same type and length). *Normalize* does the normalization function. Detail inference will be introduced in our future reports. The computed

N^* for each kind of PN-sequence is listed in Table I. Since N^* must be an integer, all the results are rounded to be integers by taking a *floor* operation.

Preliminary experiments show that, at most three or four beacon codes can be reliably detected in any position in the experiment environment as shown in Fig. 3. While in most cases, one or two beacon codes are reliably received. Even when three or four beacon codes are reliably detected, the occurrence probability of the Incidental Case is nearly zero. Since its occurrence conditions can hardly be satisfied simultaneously, whose detail explanation will be introduced in our future reports. The above conclusions are common in most indoor lighting environments, since the experiment environment is typical.

Given Table I, only those sequences with lengths over 127 can totally satisfy all cases where at most four beacon codes are detected; while those with the lengths of 31 and 63 are able to satisfy most (almost all) cases. In addition, sequences with longer length will result in much more calculation cost, since the complexity of the decomposition algorithm is $O(N_d \cdot L^2)$ where N_d is the amount of detected beacon codes. Therefore, 31-bit Gold-sequence is the optimal choice.

D. Code Selection Algorithm

The code selection algorithm is shown in Algorithm 1. Four inputs are L, N, R and T. Regarding R, the maximum repetition times is the maximum consequently repeating times of the same bit ("0" or "1") in each code. The only output is B which is the matrix of all satisfied beacon codes. As analysed in Section II-C, T is Gold-sequence here; $L = 31$.

Algorithm 1: Beacon Code Selection

```
input : L: the required length of beacon codes ;
        N: the required amount of beacon codes;
        R: the allowance of maximum repetition times;
        T: the type of required PN-sequences.
output: B: beacon codes matrix.

n = 0;
B = [ ];
while n < N do
    S0 ← GenerateNewSequence(L, T);
    if JudgeBalance(S0) = True then
        if CountRepetition(S0) < R then
            Expand B ← S0;
            n = n + 1;
        end
    end
end
```

First, potential beacon codes will be generated by `GenerateNewSequence` according to the construction of specific PN-sequence (T). Then the potential codes will be first filtered according to their balance properties, since not all the potential beacon codes are balanced by default. At the end, the maximum repetition times will be considered, since the frequency characteristics need to be largely differentiated from the frequency of ordinary light sources (i.e., unmodulated LED tubes or fluorescent tubes) to avoid their influences. Besides, if the same bit repeats too many times, the light flashing frequency will be decreased, which can result in detectable illumination flicking to human eyes.

The frequency of ordinary light sources is normally 50 Hz (the case for the experiment environment) or 200 Hz. To guarantee a reliably safe distance from the ordinary frequency and also enough number of available beacon codes, the minimum instantaneous frequency (f_i) is set to be about twice of 50 Hz, i.e., around 100 Hz. Therefore, considering the LED modulation frequency is 960 Hz, R is set to 6 ($f_i = \frac{960}{2*5} = 96$).

The selected set of 31-bit Gold-sequences are listed in Table II. Their normalized correlation peak distribution map is shown in Fig. 2. We could observe optimal auto-correlation and cross-correlation characteristics of the selected codes. Please note that there is seemingly a limitation in the amount of selected beacon codes, i.e., 12 groups. However, in practice, it is sufficient for larger space to encode lights within a neighbourhood, because the photonic diode generally has a limited angular field-of-view, such that only a limited number of light sources are directly observable.

TABLE II
THE SELECTED SET OF BEACON CODES

No.	Result Beacon Code
1	1 1 0 1 0 1 1 0 1 1 0 1 1 0 0 1 1 1 0 0 0 1 0 0 1 1 0 0 0 0 1
2	0 1 0 1 0 1 1 0 1 0 0 0 0 1 1 0 0 1 0 0 1 1 1 1 1 0 1 1 1 0 0
3	0 1 0 1 0 0 0 0 1 0 0 1 0 1 1 0 0 1 1 1 1 1 0 0 0 1 1 0 1 1 1
4	0 1 1 0 0 0 1 0 1 1 1 0 1 0 1 1 1 0 1 1 1 0 0 1 0 0 0 0 0 1 1
5	0 1 0 0 1 0 0 1 1 0 1 0 1 0 0 0 1 0 0 1 1 1 1 0 1 1 0 1 1 0 1
6	0 0 0 1 1 1 1 1 0 0 1 0 1 1 1 0 1 1 0 1 0 0 0 1 0 1 1 0 0 0 1
7	0 1 1 1 0 1 1 1 0 1 0 0 1 0 1 0 0 0 1 0 1 0 1 0 1 1 1 0 1 0 0
8	1 1 0 0 0 0 1 1 0 1 1 1 1 0 0 0 0 1 0 1 0 1 1 1 0 0 1 0 1 1 0
9	1 0 0 1 1 0 0 1 0 1 1 0 0 0 0 1 0 1 1 0 1 0 0 1 1 1 0 0 1 1 1
10	1 1 1 0 1 0 0 0 0 0 1 1 1 0 1 1 0 1 1 1 0 0 0 0 1 1 1 1 0 0 0
11	1 0 1 0 1 0 1 1 0 0 0 1 1 1 0 0 1 0 1 0 1 1 0 0 1 0 1 0 0 1 1
12	0 1 1 0 1 1 1 0 0 1 1 1 0 1 0 0 1 1 0 0 1 0 0 0 0 1 0 1 1 1 0

III. MODULATED LIGHT-SIGNAL DECOMPOSITION

The light-signal decomposition is mainly based on the optimal correlation characteristics of the selected beacon codes. With these beacon codes, the correlation response of the beacon code with the highest intensity will be the peak among all the possible correlation responses between a certain light-signal and potential beacon codes. The decomposition is achieved through iteratively extracting the intensity of the beacon code with the highest intensity in the input signal of each iteration.

The decomposition algorithm is shown in Algorithm 2. Two inputs are S_e and C. S_e is the light energy directly received by the photonic diode; C is the set of beacon codes used for light modulation. Two outputs are $Intern$ and N_d. N and L are respectively the amount and length of the beacon codes.

A. Signal Pre-processing

The received light energy signals will first be converted to amplitude signals. Before that, `EnergyCalibration` will calibrate the original energy signals to be non-negative (compatible to their physical energy). Then an amplitude filter will be used for filtering of noises produced by nature or decomposition processes. It is realized based on the balance property of the selected beacon codes. All the signals greater than 2.2 times (empirically selected) of the mean amplitude or smaller than zero are treated as noises.

B. Correlation Response and Peak Value

After the pre-processing, the correlation responses (Res) are calculated between $S_a^{'}$ and all possible beacon codes (C_f) with different bit-offsets. Based on the correlation responses,

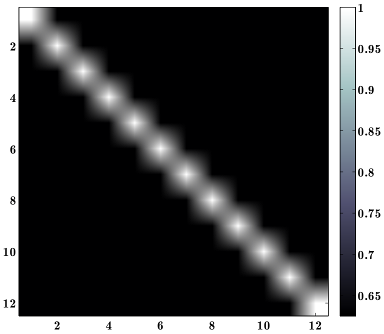

Fig. 2. The normalized peak distribution map of the selected codes. Both X and Y axes are the code order.

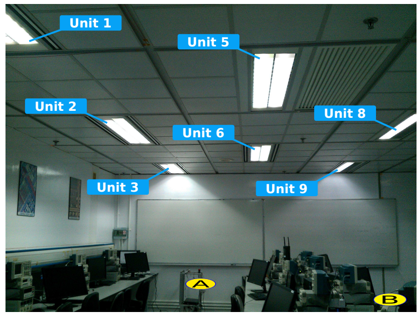

Fig. 3. The experiment environment. Position A, the validation experiments position; Position B, the sampling position of the typical waves in the larger scale validation.

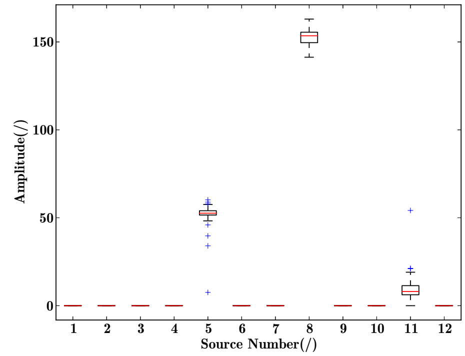

Fig. 4. The decomposition results (Boxplot) in Position B. All 12 units were powered on.

the peak value M_r, the corresponding beacon code index M_c and bit-offset M_p are computed by `FindMaxResponse`.

Algorithm 2: Light-Signal Decomposition

---

input : S_e: the received light-signals ;
C: the set of beacon codes.
output: $Inten$: the intensities of used beacon codes;
N_d: the amount of detected beacon codes.

$N, L \leftarrow$ `SizeCodeSet` $(\boldsymbol{C})$;
$N_d = 0$;
$Res = zeros(N, L)$;
$Inten = zeros(N, 1)$;
$C_f = C$;
$S_e \leftarrow$ `EnergyCalibration` (S_e);
$S_a \leftarrow$ `EnergyToAmplitude` (S_e);
for $i \leftarrow 1$ *to* N **do**
  $S_a^{'}$ = `AmplitudeFilter` (S_a);
  $Res \leftarrow$ `CorrelationCalculate` $(C_f,\ S_a^{'})$;
  $M_r, M_c, M_p \leftarrow$ `FindMaxResponse` (Res);
  $Mean_r \leftarrow \frac{(\sum_{n=1}^{L} Res(M_c)(n))-M_r}{L-1}$;
  $Inten(M_c) \leftarrow \frac{2(M_r - Mean_r)}{Ratio_r(M_c)\cdot(L+1)}$;
  $Inten(M_c), e$ = `IntenCorr` $(Inten(M_c), S_a^{'})$;
  if $\frac{e}{Inten(M_c)} > Threshold_e$ **then**
    break;
  end
  $S_c \leftarrow Inten(M_c) \cdot$ `CodeShift` $(C_f(M_c), M_p)$;
  $S_a \leftarrow S_a - S_c$;
  $C_f(M_c) \leftarrow zeros(1, L)$;
  $N_d = N_d + 1$;
end

C. Intensity Extraction of Each Beacon Code

With the peaked correlation response, the intensity of beacon code $C_f(M_c)$ can be decomposed by:

$$Inten(M_c) = \frac{2(M_r - Mean_r)}{Ratio_r(M_c) \cdot (L+1)} \quad (2)$$

where $Mean_r$ is the mean of all the other responses between $S_a^{'}$ and $C_f(M_c)$ except M_r. $Ratio_r(M_c)$ is the difference between the peak and mean of others of the normalized auto-correlation responses of $C_f(M_c)$. It precisely holds only when there is only one modulated light source ($n = 1$). Detail inference will be introduced in our future reports.

For the case with multiple light sources, the closer the intensities of other beacon codes are to the highest intensity, the bigger the error of the intensity extracted by equation 2 is. Besides, numerous errors might also be introduced by environment lights. Although the errors can be largely reduced by the mean calculation, the precision cannot be guaranteed. Regarding this, the extracted $Inten(M_c)$ will be corrected by minimizing the error between the decomposed signal and corresponding original signal, through `IntenCorr`.

If $\frac{e}{Inten(M_c)} > Threshold_e$, the extracted $Inten(M_c)$ is treated as an unreliable result to be excluded. The decomposition will not stop until no more beacon code can be reliably decomposed. At the end, the intensities of inclusive beacon codes ($Inten$) and the amount of exactly detected beacon codes (N_d) are returned. Those beacon codes without exact intensities are treated as unreceived or unobservable. Their intensities will be set to zeros. The complexity of the light-signal decomposition algorithm is $O(N_d \cdot L^2)$.

IV. Validation and Analysis

A. Experiment Environment

The VLC-based indoor localization system is installed in the experiment environment as shown in Fig. 3. There are 12 modulated LED sources (units, Unit 1-12) in the environment. Only seven of them can be seen in Fig. 3, i.e., Unit 1, 2 , 3, 5, 6, 8 and 9. They are all modulated with the selected beacon codes listed in Table II. The proposed code selection and light-signal decomposition algorithms are implemented on a tablet connected with a photonic diode.

B. Validation Experiments

For stability and accuracy concerns, the decomposition results (intensities) under the same situation (e.g., same position and orientation, same light conditions, etc) should have small variance δ^2 and error e. Validation experiments were performed at the fixed Postion A as shown in Fig. 3, including intensity ground-truth measurements and mixed lights decomposition experiments.

Intensity ground-truth can hardly be directly measured by sensors, because it represents light amplitude, not light energy. Thus, the intensity ground-truth from each single light source in Position A was measured using the decomposition algorithm described in Section III. To minimize the influences from other light units, only the unit being measured was turned on. Besides, during the measurements, the photonic diode was always with the same orientation. The measurement duration of each unit is 100 s, during which at least 110 groups of data were gathered. The mean of the intensities is treated as the intensity ground-truth ($I_{standard}$).

Given the intensity ground-truth measurements, only the lights from the nearest three units (i.e., Unit 2, 3 and 6) can be reliably detected in Position A. Thus, for the mixed

TABLE III

DECOMPOSITION PERFORMANCE OF DIFFERENT ALGORITHMS IN DIFFERENT SITUATIONS

Unit	$I_{standard}$ Each Single		$I_{optimal\_decomp}$ Unit 2+3			Unit 2+6			Unit 3+6			All Three			I_{naive_decomp} All Three		
	μ	δ^2	μ	δ^2	$\mu_e/\%$	μ	δ^2	$\mu_e/\%$	μ	δ^2	$\mu_e/\%$	μ	δ^2	$\mu_e/\%$	μ	δ^2	$\mu_e/\%$
2	3.44	0.31	3.85	0.70	11.9	2.97	0.36	13.8	-	-	-	0.82	0.89	76.2	-	-	-
3	11.22	1.22	11.28	1.37	0.5	-	-	-	9.93	1.35	11.5	9.42	1.67	16.1	16.46	8.55	46.7
6	18.79	2.05	-	-	-	17.83	1.41	5.1	17.72	2.10	5.7	16.37	2.03	12.9	29.75	3.89	58.4

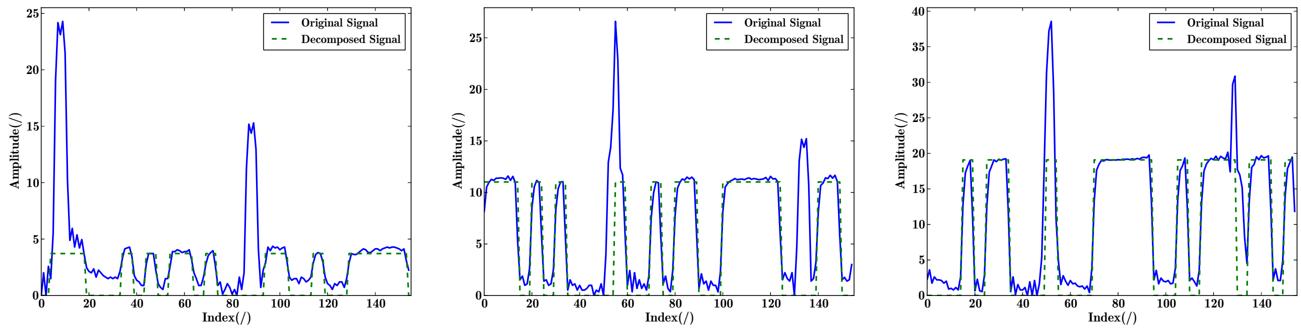

(a) Decomposition results of Source 2 (Unit 2) (b) Decomposition results of Source 3 (Unit 3) (c) Decomposition results of Source 6 (Unit 6)

Fig. 5. The decomposition results of each single unit in Position A

lights decomposition experiments, there are three 2-mixture situations (i.e., Unit 2+3, Unit 2+6 and Unit 3+6) and one 3-mixture situation (i.e., Unit 2+3+6). For each test, only the testing units were powered on. In addition, a decomposition comparison experiment was carried out between the proposed decomposition method and a naive decomposition method, using the same dataset. Compared with the proposed decomposition algorithm, the naive decomposition algorithm do not conduct energy calibration, amplitude filter and intensity correction functions.

C. Results and Analysis

The experiments results are shown in Table III. The typical original and decomposed waveforms in the intensity ground-truth measurements are shown in Fig. 5. The two highest peaks of each original signal in Fig. 5 were produced by an external *motion tracking system*, which was used to measure the position of the photonic diode. Fig. 5 shows that, the decomposed signals match the original signals very well. During the intensity ground-truth measurements, the decomposed signals can always match the original signals precisely, which indicates that the proposed decomposition algorithm can precisely extract the intensity of each beacon.

In Table III, μ and δ^2 are the mean and variance of intensities, which are computed by fitting a normal distribution. μ_e is the mean of the error rate of the decomposed intensities ($I_{decomposed}$), which is calculated by equation 3.

$$\mu_e = \frac{|I_{decomposed} - I_{standard}|}{I_{standard}} \cdot 100\% \qquad (3)$$

According to the results, for the 3-mixture situation (All Three), both the μ_e and δ^2 of $I_{optimal\_decomp}$ are much less than those of I_{naive_decomp}. The naive decomposition algorithm can only decompose two beacon codes. While the algorithm proposed in Section III can decompose all those three beacon codes with the correct ranking of the intensities.

For the 2-mixture situations, their values of μ_e are all smaller than that for All Three ($I_{optimal\_decomp}$). Especially for the intensity of Unit 2, the stronger the other signals are, the greater the μ_e of Unit 2 is. It is because the intensity of Unit 2 is comparatively much lower than those of Unit 3 and 6. This indicates that, except for too weak signals the proposed decomposition algorithm can relatively precisely decompose mixed light-signals in most cases. Although the μ_e can be 16.1%, it is still sufficient for the entire indoor localization system which localizes based on posterior maximum likelihood using a Bayesian filter.

All the variances of $I_{optimal\_decomp}$ are almost the same as those of $I_{standard}$, respectively. This indicates that the stability of the proposed decomposition algorithm maintains well in most cases. Even though the variances include not only the uncertainty of the proposed decomposition algorithm, but also the uncertainty of the light-signals, they still satisfy the requirements of the proposed indoor localization system.

D. Larger Scale Validation

To validate the selected beacon codes and proposed decomposition algorithm in a larger scale, the same validation experiments were performed in a larger environment, i.e., the entire range as shown in Fig. 3. During the experiments, all the 12 LED units were powered on. The typical case of the decomposed results is shown in Fig. 4, which indicates the case in Position B as shown in Fig. 3. The corresponding decomposition processes are shown in Fig. 6.

In Fig. 6, after energy calibration, the energy signal from the photonic diode was converted into the amplitude signal. According to the comparison of the original amplitude signal and the signal reconstructed from the decomposed component-signals in Fig. 6, the two signals match well, except for natural noises. In Fig. 4, the distributions of the decomposed three beacon codes (Unit 5, 8 and 11) are all concentrated. The well-matched results and concentrated distributions indicate the feasibility and stability of the proposed method in the entire experiment environment.

V. LOCALIZATION TEST

With the selected beacon codes and the proposed decomposition algorithm, localization tests were made in the

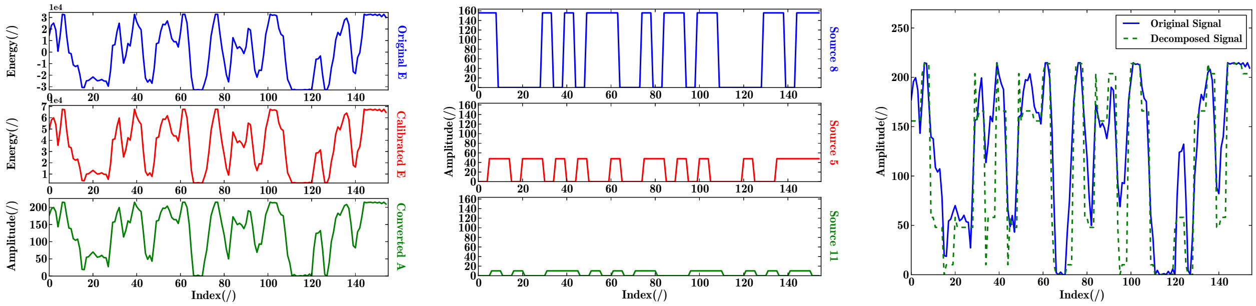

(a) Pre-processing (b) Decomposed component-signals (c) Reconstructed signal

Fig. 6. The light-signal decomposition processes in Position B. The photonic diode was straight up. All the 12 modulated LED units were powered on.

experiment environment as shown in Fig. 3. Firstly, training datasets for the GPR-based map generation were gathered in the experiment environment. In the training datasets, the position data use the SLAM results from a test mobile robot. Then the 2D-intensity-distribution-map-group (including the mean and the variance) of each modulated LED unit was generated through GPR, using the training datasets.

Based on these maps, the VLC-based indoor 2D-localization tests were done under the following conditions:

- All the units in the experiment environment were powered on and worked well.
- The tablet worked at the height around 1.2 m off the ground which is the average height for a hand-held device in-use. The orientation of the photonic diode was roughly the straight up direction without strict requirements. Both the height and orientation were arbitrarily changed slightly by fitting to a normal use-case.
- The test covered all available areas in the environment.

Given more than 1000 groups of localization results, the mean and standard deviation of localization errors (by Euclidean distance) are respectively 0.56 m and 0.476 m. This accuracy is much higher than the best result achieved by WiFiSLAM (3 m) [6]. It is even sufficient for the localization and navigation of service robots. The average required time for processing each frame is 20 ms. A video supplementary is attached to show the high performance of the proposed framework with real experiments. More detail results of the localization tests will be discussed in our future reports.

VI. Conclusion and Future Work

In this paper, a real-time asynchronous blind light-signal decomposition method and a corresponding tiny-length code selection method are introduced for VLC-based indoor localization system. The light-signal decomposition results indicate that the proposed method can precisely and stably extract the intensity data of each reliably received beacon code. The VLC-based indoor localization system developed based on the proposed encoding and decomposition method can achieve an accuracy of 0.56 m which is the-state-of-the-art of its kind. However, further research is necessary for the adaption of the system in larger and more challenging scenarios. The future work will consider influences from sensor orientation in 3D-space, noise influences, and beacon grouping, etc.

Video Supplement

The attached video shows the dynamic localization results of the entire VLC-based indoor localization system in the experiment environment as shown in Fig. 3.

References

[1] M. Liu, B. T. Alper, and R. Siegwart, "An adaptive descriptor for uncalibrated omnidirectional images - towards scene reconstruction by trifocal tensor," in *IEEE International Conference on Robotics and Automation, 2013*, 2013.

[2] M. Liu, C. Pradalier, and R. Siegwart, "Visual homing from scale with an uncalibrated omnidirectional camera," *IEEE Transactions on Robotics*, vol. 29, no. 6, pp. 1353–1365, Dec.2013.

[3] R. Arroyo, P. F. Alcantarilla, L. M. Bergasa, J. J. Yebes, and S. Gámez, "Bidirectional loop closure detection on panoramas for visual navigation," in *Intelligent Vehicles Symposium Proceedings, 2014 IEEE*. IEEE, 2014, pp. 1378–1383.

[4] R. Arroyo, P. F. Alcantarilla, L. M. Bergasa, J. J. Yebes, and S. Bronte, "Fast and effective visual place recognition using binary codes and disparity information," in *Intelligent Robots and Systems (IROS 2014), 2014 IEEE/RSJ International Conference on*. IEEE, 2014, pp. 3089–3094.

[5] R. W. Wolcott and R. M. Eustice, "Visual localization within lidar maps for automated urban driving," in *Intelligent Robots and Systems (IROS 2014), 2014 IEEE/RSJ International Conference on*. IEEE, 2014, pp. 176–183.

[6] B. Ferris, D. Fox, and N. D. Lawrence, "Wifi-slam using gaussian process latent variable models." in *IJCAI*, vol. 7, 2007, pp. 2480–2485.

[7] Y. X. Sun, M. Liu, and Q.-H. Meng., "Wifi signal strength-based robot indoor localization," in *IEEE International Conference on Information and Automation*, 2014.

[8] T. Komine and M. Nakagawa, "Fundamental analysis for visible-light communication system using led lights," *Consumer Electronics, IEEE Transactions on*, vol. 50, no. 1, pp. 100–107, 2004.

[9] A. Jovicic, J. Li, and T. Richardson, "Visible light communication: opportunities, challenges and the path to market," *Communications Magazine, IEEE*, vol. 51, no. 12, pp. 26–32, 2013.

[10] M. Liu, K. Qiu, S. Li, F. Che, L. Wu, and C. P. Yue, "Towards indoor localization using visible light communication for consumer electronic devices," in *Proceedings of the IEEE/RSJ International Conference on Intelligent Robots and Systems (IROS)*, Chicago, the USA, 2014.

[11] F. J. MacWilliams and N. J. Sloane, "Pseudo-random sequences and arrays," *Proceedings of the IEEE*, vol. 64, no. 12, pp. 1715–1729, 1976.

[12] G. J. Ness and T. Helleseth, "Cross correlation of m-sequences of different lengths," *IEEE transactions on information theory*, vol. 52, no. 4, pp. 1637–1648, 2006.

[13] R. Gold, "Maximal recursive sequences with 3-valued recursive cross-correlation functions (corresp.)," *Information Theory, IEEE Transactions on*, vol. 14, no. 1, pp. 154–156, 1968.

[14] D. V. Sarwate and M. B. Pursley, "Crosscorrelation properties of pseudorandom and related sequences," *Proceedings of the IEEE*, vol. 68, no. 5, pp. 593–619, 1980.

[15] A. Goldsmith, *Wireless communications*. Cambridge university press, 2005.

[16] R. Gold, "Optimal binary sequences for spread spectrum multiplexing (corresp.)," *Information Theory, IEEE Transactions on*, vol. 13, no. 4, pp. 619–621, 1967.